OPTICAL PROPERTIES OF SIGNIFICANT ACOUSTO-OPTIC CRYSTALS

V. Musinschi[a], M. Caraman[b], C. Musinschi[c], N. Syrbu[c]

[a]*Free International University of Moldova, 52, Vlaicu Pircalab str., MD-2012, Chisinau, Moldova*
[b]*Moldova State University, 60, A. Mateevici str., MD-2009, Chisinau, Republic of Moldova*
[c]*Technical University of Moldova, 168, Stefan cel Mare ave., MD-2004, Chisinau, Republic of Moldova*

(Received 25 September 2008)

Abstract

Results of the investigation of spectra in the energy ranges of fundamental absorption of $PbMoO_4$ crystals in two radiation polarizations $(E \parallel C_4)$ and $(E \perp C_4)$ of incident light in the 77-300 K temperature range are presented. Possibilities of the interpretation of particularity of absorption spectra on the basis of the proposed band structure are examined. Analysis of measurement results for reflection spectra of paratellurite TeO_2 and wulfenite $(PbMoO_4)$ crystals within the interval 50-1000 cm^{-1} is presented. The Kramers–Kronig method is used to interpret the peculiarities of reflection spectra. The calculus of reflection spectra is made by the multioscillation model.

The interest in the study of the optical properties of TeO_2 and $PbMoO_4$ crystals is determined not only by the fundamental physical mechanisms present in these materials but also by a wide spectrum of possible applications in high-speed acousto-optic devices that perform spatial, temporal, and spectral modulation of optical beams.

A description of experimental results of studying the optical properties of tetragonal TeO_2 (class 422) and $PbMoO_4$ (class 4/m) crystals is given. The phenomena usually studied to obtain information on the optical properties of crystals are absorption and reflection in a large wavelength range.

1. The fundamental absorption of PbMoO4 crystals

Optical measurements have many unique and attractive features for studying and characterizing crystal properties. They are contactless nondestructive and compatible with any transparent ambient, including high-vacuum environments, and useful for in-situ analysis in processing systems.

Wulfenite crystals $PbMoO_4$ are the crystalline materials that include manufactured crystals and naturally accruing minerals. They have high photosensitivity in blue region of spectra [1].

In the presented study, we used $PbMoO_4$ crystals being of the C_{2h}^5 space-symmetric group obtained through extraction from melt according to the Chochralski method mainly to [100] direction having the lattice parameters a = 5.4312 Å and c = 12.08 Å. In references [2-3], these crystals are being known as uniaxially negative crystals of light yellow color with high acousto-optic figures of merit

$$M_2 = \frac{n^6 p^2}{\rho v^3} \tag{1.}$$

This part of the study presents the experimental results of studying optical absorption at fundamental absorption of $PbMoO_4$ crystals in two radiation polarizations $(E \parallel C_4$ and $E \perp C_4)$.

The transmission of a thin slab of known thickness, together with the absolute reflectivity at nearly normal incidence, was measured. The optical measurements were carried out in the temperature range from liquid nitrogen to room temperature. The samples with a thickness of 10-30 μm were used for transmission spectrum.

In our study, two types of plates were used: (1) plates in which the developed faces contained the C_4-axis and (2) plates in which the developed faces were perpendicular to the C_4-axis.

Optical measurements of transmission and reflectivity were performed at nearly normal incidence by spectrophotometer set-up mounted on the basis of an MDR-3 monochromator. The absorption coefficient α was calculated by the following relationship

$$\alpha = \frac{(1-R)^2 e^{-\alpha d}}{1 - R^2 e^{-2\alpha d}} \qquad (2)$$

For a nonzero momentum matrix element which determines the transition probability between the bands of crystals, a simple model of band structure gives for alloyed direct transition (with approximate conservation of the electron wave vector)

$$\alpha \hbar \omega = C_d \, (\hbar \omega - E_g^d)^{1/2}. \qquad (3)$$

Coefficient C_d involves constant valence- and conduction-band effective masses and matrix element of transition. E_g^d is the optical edge at the temperature of measurements. For $PbMoO_4$ crystals at T= 300 K it is 3.28 and 3.36 eV, respectively.

Figure 1 shows the spectral variation of the absorption coefficient for pure $PbMoO_4$ at a temperature of 218 and 77 K. Below ~10^3 cm^{-1}, the absorption decreases with increasing λ much more slowly than predicted in relationship (3). In this region, electron cannot make a direct transition from the top of the valence band to the bottom of the conduction band; this would violate conservation of momentum. The $ℏω_f$ is the energy of particle involved in optical transition which can be generated or absorbed in it. In this case, probability depends not only on the density of states and the electron–phonon matrix elements as in the direct case but also on the electron–phonon interaction which is temperature dependent.

In this energy region the *indirect transitions* are achieved with

$$\alpha \hbar \omega = C_{ind} \, (\hbar \omega \pm \hbar \omega_f - E_g^{ind})^2, \qquad (4)$$

where $\hbar \omega_f$ is the energy of phonon participant in the indirect transition, E_g^{ind} is the energy interval between the valence and conduction bands (*indirect edge*). As seen in Fig. 1a, at the lowest energies, α rises due to the onset of the indirect absorption by the $(\alpha \hbar \omega)^{1/2}$ dependence on photon energy.
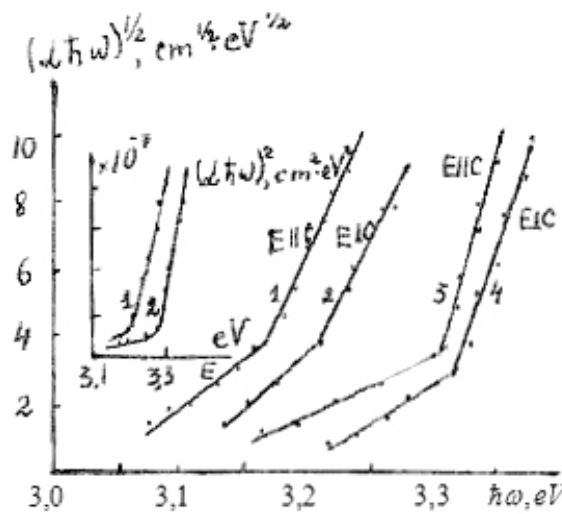

Fig. 1. $(\alpha ℏ\omega)^2$ and $(\alpha ℏ\omega)^{1/2}$ spectra of $PbMoO_4$ crystals.
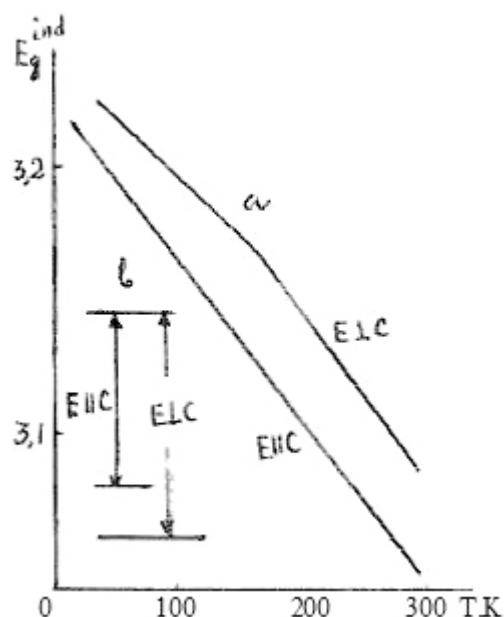
187

Fig. 2. Temperature depends of E_g^{ind} of PbMoO$_4$.

By extrapolating the linear region of curves to the value $\alpha = 0$ in two types of transitions minimum energy gaps of 3.2 and 3.23 eV at 77 K for E $\parallel$ C$_4$ and E $\perp$ C$_4$ were obtained.

The slope of decrease of the lowest energy section of $(\alpha\hbar\omega)^{1/2}$ with temperature was obtained.

It is explained by phonon density diminution at low temperature. Both indirect (a) and direct (b) absorption edge data are presented in Fig. 1a. As is shown in this figure, the dependence $\alpha = f(\hbar\omega)$ in the lowest energy range of absorption is described by the expression

$$\alpha\hbar\omega = C_1^{ind}(\hbar\omega + \hbar\omega_f - E_g^{ind})^2 + C_2^{ind}(\hbar\omega - \hbar\omega_f - E_g^{ind})^2. \qquad (5)$$

The thermal bias of the curves towards lower energies of photons was observed, which is attributed to the temperature change in the interband space (the interval between the valence and conduction bands).

Figure 2a shows the temperature dependence of E_g^{ind} for E $\parallel$ C$_4$ and E $\perp$ C$_4$. The model of the energy state arrangement in the PbMoO$_4$ crystals which provides a relevant description of optical transitions is proposed schematically in Fig. 2b, in which the positions of the valence band top and the conduction band count in favor of direct and indirect optical transitions between them.

2. Infrared reflection of TeO$_2$ and PbMoO$_4$ crystals

2.1. In optics, it is frequently convenient to define a complex refractive index $\overline{n}$ through the square root of the complex dielectric constant

$$\varepsilon(\omega) = \varepsilon_1(\omega) - i\,\varepsilon_2(\omega), \qquad (6)$$

$$\overline{n} = n - i\kappa = \sqrt{\varepsilon} = \sqrt{\varepsilon_1 - i\varepsilon_2}, \qquad (7)$$

and

$$\varepsilon_1 = n^2 - \kappa^2, \quad \varepsilon_2 = 2n\kappa, \qquad (8)$$

where "n "is the real index of refraction and "κ " is the index of absorption.

The refractive index "n " gives the phase shift of the optical wave, and the extinction coefficient "κ " gives the attenuation of the wave.

The optical properties of insulators as the semiconductors are often subdivided into the ones of electronic nature and the ones of lattice nature. The lattice properties concern processes involving vibrations of the lattice (absorption and creation of phonons).

The reflection and transmission from a surface are given by

$$r = \frac{(\bar{n}-1)}{(\bar{n}+1)} = |r|\exp(i\theta) = \left|\frac{n-1-i\kappa}{n+1-i\kappa}\right|,$$

(9)

θ is the shift of the incident and reflected waves,

$$R = |r^2|$$

(10)

and T = 1 – R, where R and T are the reflectance and transmission.

From (9), we obtain

$$R = |r^2| = \frac{(n-1)^2 + k^2}{(n+1)^2 + k^2}$$

(11)

and

$$tg\theta = \frac{2nk}{n^2 + k^2 - 1}.$$

(12)

From solution of (11) and (12), it follows

$$n = \frac{1-R}{1+R-2\sqrt{R}\cos\theta}$$

(13)

and

$$\kappa = \frac{2\sqrt{R}\sin\theta}{1+R-2\sqrt{R}\cos\theta}.$$

(14)

An expression of practical utility is the one in which the experimentally measured power reflection R at normal incidence is explicitly displayed as shown

$$\theta(v) = \frac{\upsilon}{\pi} P \frac{\ln R(\upsilon^1) d\upsilon^1}{(\upsilon^1)^2 - \upsilon^2}$$

(15)

and may be found by the Kramers–Kronig analysis.

If R(v) can be measured only in a limited frequency range Δv = v_B – v_A but extrapolations can be made to establish reasonable values of "n" and "k"

$$\theta(v) = \theta_1(v) + \theta_2(v) + \theta_3(v),$$ (16)

where

$$\theta_1(v) = -\frac{\upsilon}{\pi} P \int_0^{\upsilon_A} \frac{\ln R(\upsilon^1) d\upsilon^1}{(\upsilon^1)^2 - \upsilon^2},$$

(17)

$$\theta_2(v) = -\frac{\upsilon}{\pi} P \int_{\upsilon_A}^{\upsilon_B} \frac{\ln R(\upsilon^1) d\upsilon^1}{(\upsilon^1)^2 - \upsilon^2}$$

(18)

and

$$\theta_3(v) = -\frac{\upsilon}{\pi} P \int_{\upsilon B_A}^{\infty_B} \frac{\ln R(\upsilon^1) d\upsilon^1}{(\upsilon^1)^2 - \upsilon^2}.$$

(19)

Results of measurement of reflection spectra of paratellurite TeO$_2$ crystals within the interval from 0.2 to 50 μm have been analyzed.

Figure 3a shows the spectral variation of the reflection coefficient R and the phase shift "θ" of TeO_2 crystals for two radiation polarizations $E\parallel C_4$ and $E\perp C_4$. The frequency dependence of phase shift θ(ν) reflects the structure of vibrational spectra.
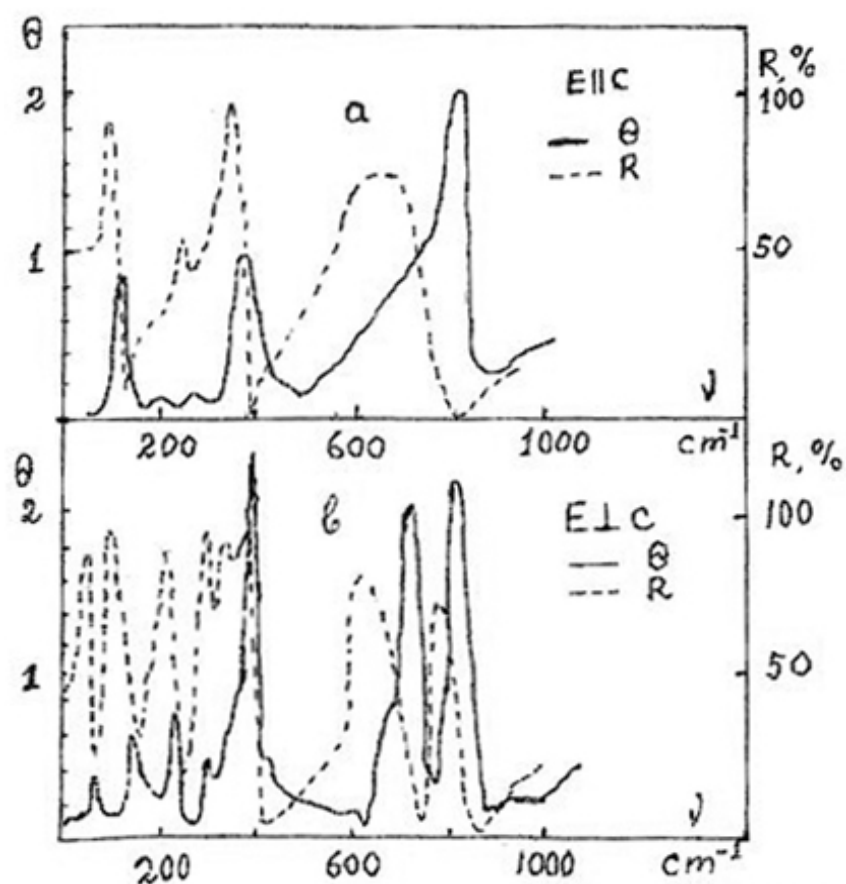

Fig. 3. Reflection spectra R and spectral variation of phase shift θ of TeO_2: a) $E\parallel C$ and b) $E\perp C$.

In TeO_2 crystal, atoms are attached by four neighboring "O" atoms which are arranged in the peaks of triangular bipyramids.

A group theory analysis determines number of the lattice vibration contributions to the dielectric constant ε(ω). In the center of the Brillouin zone ($\vec{k} = 0$) [4, 5]

$$\Gamma = 4\, A_1(R) + 4\, A_2(IR, E\parallel C) + 5\, B_1(R) + 4\, B_2(R) + 8\, E\, (IR, E+\perp C) \qquad (20)$$

The relevant absorption peaks of κ(ν) are listed in Table 1.

Table 1. Peaks of absorption in TeO_2 crystals [6].

Peak	$E\parallel C_4$				$E\perp C_4$							
	1	2	3	4	1	2	3	4	5	6	7	8
ν cm^{-1}	81	252	315	567	123	164	205	293	-	327	623	754

Four bands in the spectrum θ(ν) in $E\parallel C_4$ and seven bands in $E\perp C_4$ were found. Positions of absorption peaks are listed in Table 1.

Figure 4 presents frequency dependences of $\varepsilon_1(\nu)$ and $\varepsilon_2(\nu)$ of crystals TeO_2 on $E\parallel C_4$ and $E\perp C_4$. Results of calculations are shown in Table 2.
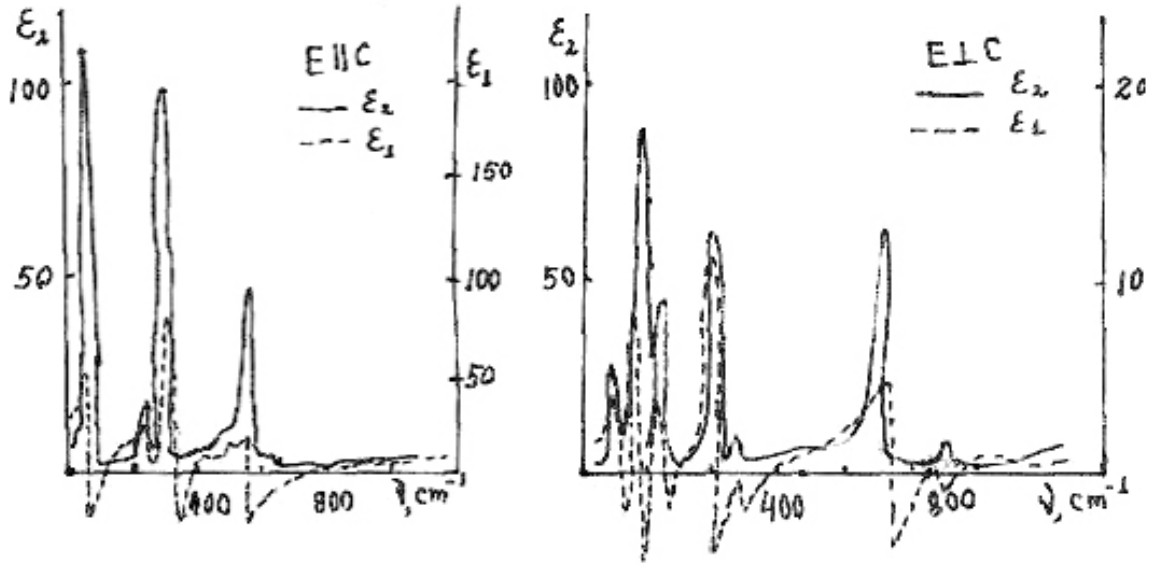
Fig. 4. Frequency dependences of $\varepsilon_1(v)$ and $\varepsilon_2(v)$ on $E\parallel C$ and $E\perp C$ for TeO_2.

Table 2. Frequency dependence of $\varepsilon_1(v)$ and $\varepsilon_2(v)$.

$E\parallel C_4$			$E\perp C_4$		
v (cm^{-1})	ε_1	ε_2	v (cm^{-1})	ε_1	ε_2
81	- 39	141	123	- 36	191
253	29	21,53	164	- 84	46
315	- 132	118	205	- 20	52
567	- 34	63,27	286	- 15	
			303	- 19	
			623	- 63,51	30
			754	- 12,84	

2.2. The infrared reflection spectra of $PbMoO_4$ crystals were also measured. Four frequencies of active phonons in 369–50 cm^{-1} and in 700–900 cm^{-1} are determined.

Figure 5 shows the spectral variation of the reflection spectra and $\varepsilon_1(v)$ and $\varepsilon_2(v)$ calculations in the polarization $E\parallel C_4$.

The peculiarities of IR reflection spectra were interpreted in terms of the theoretical-group analysis of 4/m (C_{2h}^5) point symmetry group of $PbMoO_4$ crystals.

In the center of the Brillouin zone ($\vec{k}=0$) the following Raman and IR lattice vibration are found [7, 8]

$$\Gamma_{opt} = 3\,A_g + 5\,A_u + 5\,B_g + 3\,B_u + 5\,E_g + 5\,E_u \qquad (21)$$

The mechanism of interaction between electromagnetic radiation and acoustic wave is the coupling between the electromagnetic field with vibrations of an ionic lattice; it may be described by treating the solid to be a collection of damped harmonic oscillators with a characteristic vibrational frequency ω_{TO} and damping constant γ.

In the case of more than one characteristic vibrational frequency, the dielectric function $\varepsilon(\omega)$ may be written as

$$\varepsilon(\omega) = \varepsilon_\infty + \sum_{j=1}^{N} \frac{S_j\left(\omega_{TO}^j\right)^2}{\left(\omega_{TO}^j\right)^2 - \omega^2 - i\omega\gamma_j}, \qquad (22)$$

S_j is the oscillator strength of j–oscillator,

$$S_j = \frac{4\pi N_j e_j^2}{m_j}, \tag{23}$$

where e_j is the phenomenological ionic change of j–oscillator, N_j is the number of oscillator per unit volume, m_j is its reduced mass, and ω^j_{TO} is the characteristic vibrational frequency. This model assumes no coupling between modes and provides a good representation of the dielectric constant, especially if the modes are weak (small separation between ω_{TO} and ω_{LO}) and uncoupled. ω_{TO}, ω_{LO}, and γ are the characteristic transversal and longitudinal vibrational frequencies and damping coefficient of oscillators.
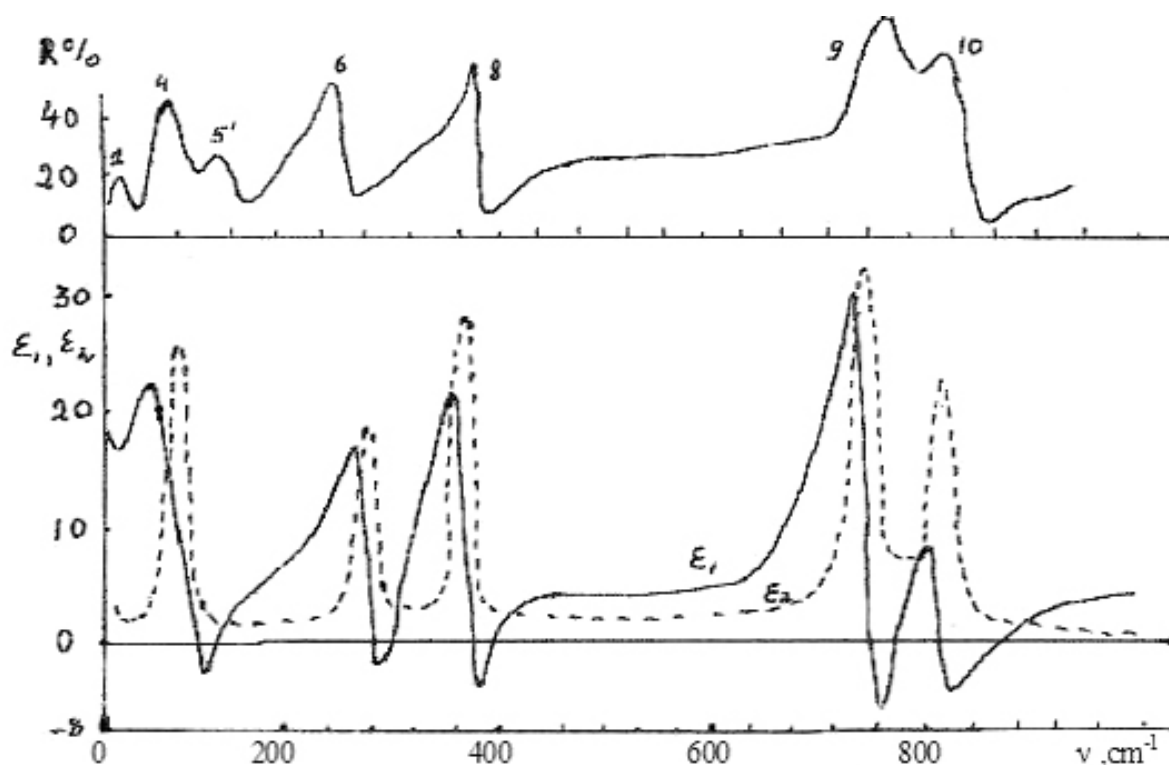

Fig. 5. Reflection spectrum R and $\varepsilon_1(\nu)$, $\varepsilon_2(\nu)$ calculations in $E\parallel C_4$ for PbMoO$_4$.

As is shown in Fig. 5, the IR reflection spectrum contains six active phonons (bands 1, 4, 5, 8, 9, 10), which correspond to the A_u symmetry ($E\parallel C_4$ polarization). In the $E\perp C_4$ polarization (Fig. 6), six phonons (bands 2, 3, 5, 7, 9, 10) which correspond to the B_u symmetry are observed.
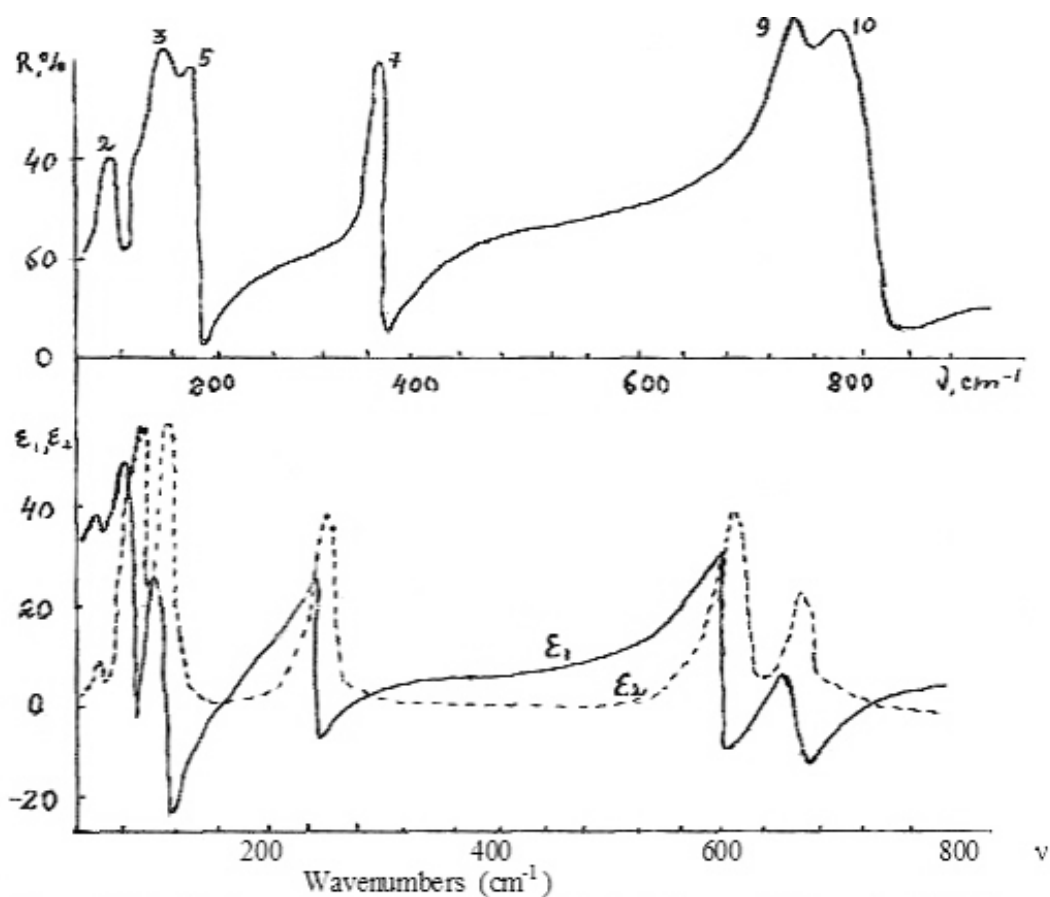
The parameters of phonons were found from an outline calculation in accordance with the dispersion relation

$$\varepsilon(\omega) = \varepsilon_1(\omega) - i\,\varepsilon_2(\omega) = \varepsilon_\infty + \sum_{j=1}^{N} \frac{\varepsilon_\infty\left(\omega^2 - \omega^2_{Ij}\right)}{\omega^2_{Tj} - \omega^2 - i\omega\gamma_j} \tag{24}$$

at a complete coincidence of measured reflection spectrum $R(\omega)$ with the one calculated in accordance with (24).

The IR reflection spectrum, $\varepsilon_1(\omega)$ and $\varepsilon_2(\omega)$ of PbMoO$_4$ crystals for $E\perp C_4$ are shown in Fig. 6.

Characteristics of phonons in the two polarizations of incident light are listed in Table 3.

Fig. 6. IR reflection spectrum R and $\varepsilon_1(\nu)$, $\varepsilon_2(\nu)$ calculations in $E \perp C_4$ for PbMoO$_4$.

Table 3. Parameters of lattice vibrations in PbMoO$_4$.

Polarization	Modes j	ν^j_{TO} cm^{-1}	ν^j_{LO} cm^{-1}	$\nu^j_{LO} - \nu^j_{TO}$ cm^{-1}	γ_j
E∥C$_4$	1	58,1	66,0	7,9	13,0
	4	109	139	20	20,0
	6	258,9	277,5	18,6	13,6
	8	368,7	384	15,3	6,9
	9	766	814	48	16,0
	10	827	868	41	17,0
E⊥C$_4$	2	75,7	79,1	3,4	5,1
	3	108	128	20	17
	5	139	156	17	12
	7	298	313,6	15,6	5,6
	9	760	835	75	21
	10	818	891	73	20

Considering the value of masses of vibrating atoms in the PbMoO$_4$ lattice and the nature of the chemical bond, one can divide vibration modes into "inner" and "external". Strong bond of the atoms in tetrahedron MoO$_4^{2-}$ contributes to occurrence of high-frequency vibrations. Bands 9 and 10 are the ones considered as inner vibrations at high frequency. These phonons occur in both polarizations of IR-spectra and have the same nature as those in RD

861-871 cm^{-1} (A$_g$) and 785-772 cm^{-1}(B$_g$) [2, 9]. In the range 760–369 cm^{-1} IR reflection bands do not occur, but one can see the polarization structure in the range 369-50 cm^{-1}.

Low-energy bands (250-50 cm^{-1}) could be explained by Pb^{2+} and MoO$_4$ vibrations one against another. The maximum value of oscillator strength occurs for bands 3, 4, and 5. Hence, 1, 4 and 2, 3 band groups are determined by inner vibration in the MoO$_4$ tetrahedron. The 700-900 cm^{-1} bands occur in both polarizations and correspond to O–O interaction.

References

[1] V. Musinschi, M. Caraman, A. Macarenco, USSR J. Appl. Spect., 48, 5, 839, (1988).
[2] G. Berny, P. Bourgion, B. Aurault, Optics Communications, 6, 4, 383, (1972).
[3] G. Bahshiev, A. Morozov, USSR Optic.-mechan. industry, 9, 742, (1977).
[4] D.M. Korn, A.S. Pine, G. Dresselhaus and T. Reed, Phys. Rev. B, 8, 3, 768, (1973).
[5] A.S. Pine and G. Dresselhaus, Phys. Rev. B, 5, 4087, (1972).
[6] M. Caraman, V. Musinschi, Iu. Smirnov, URSS J.P.S, 48, 5, 825, (1988).
[7] D.A. Pinnow, L.G. Van Uitert, A.W. Warner, Appl. Phys. Lett., 15, 1, 83, (1969).
[8] M. Caraman, V. Musinschi, N. Syrbu, S. Hachaturova, URSS Sol. Stat. Phys., 33, 4, 1314, (1991).
[9] G.M. Loiacono, I.F. Balasico, R. Bonner, J. Cryst. Growth, 5, 21, 1, 1, (1974).